Buttwelding of Mg-Cu-Gd Bulk Metallic Glass using a High-brightness Fiber Laser†

TERAJIMA Takeshi*, KIMURA Hisamichi** and INOUE Akihisa***

Abstract

The light metal based metallic glass $Mg_{65}Cu_{25}Gd_{10}$ has low specific gravity and excellent mechanical properties and thus is expected to be a useful structural material. However, welding of $Mg_{65}Cu_{25}Gd_{10}$ is difficult since it immediately crystallizes if the quench rate is lower than the critical value. In this study, a high-brightness fiber laser with an ultrahigh power density of several megawatts per square millimeter, which corresponds to the power density of an electron beam and is a well suited for this purpose, is examined for welding $Mg_{65}Cu_{25}Gd_{10}$. The laser beam was transmitted through an optical fiber and focused on the butt surface of the $Mg_{65}Cu_{25}Gd_{10}$ rods that were synchronously rotated at 3000 rpm at 0.5 MPa. The molten alloy that forms following laser irradiation was extruded from the joint, and the specimens were successfully welded. The microstructure observed by micro-focus X-ray diffraction showed that the crystalline phase was not present inside the joint but was in the extruded region. The success of the proposed welding is likely attributable to the pressure applied to the specimens, which plays an important role in extruding the crystalline phase from the joint.

KEY WORDS: (Mg-based metallic glass), (fiber laser), (buttwelding)

1. Introduction

Metallic glass possesses unique properties such as high mechanical strength, low elastic coefficient, small solidification shrinkage, and high resistance to corrosion. These properties originate from its amorphous structure and are not found in crystalline metals. Usually, various metallic glasses exhibit a large viscous flow at the supercooled liquid region. The utilization of the flow enables the fabrication of metallic glasses in the form of three-dimentional shapes such as semi spheres and small gears[1)]. These features open up new areas of applications of bulk metallic glass, as materials for mechanical structural parts, sporting goods, optical precision parts and cutting tools[2)].

Some types of metallic glass, such as Mg-[3)], Zr-[4,5)], Fe-[6,7)], Pd-[8)], and Ni-based[9)] alloys, have low critical cooling rates. $Mg_{65}Cu_{25}Gd_{10}$, in particular, has one of the lowest critical cooling rates of only 1 K/s[10)]. The strong glass-forming ability of $Mg_{65}Cu_{25}Gd_{10}$ allows the fabrication of amorphous alloy rods with a maximum diameter of 8 mm[10)]. In addition, the specific strength of $Mg_{65}Cu_{25}Gd_{10}$ is twice that of typical AZ91 Mg alloy. Therefore, $Mg_{65}Cu_{25}Gd_{10}$ is expected to be used as a lightweight structural material such as for vehicle bodies and car appliances. However, it is necessary to develop joining techniques for metallic glass in order to broaden the scope of its industrial applications. There have been attempts to join pieces of Zr-based metallic glass using electron beam welding, explosive welding, pulse current welding, friction welding[11-13)], and laser welding[14,15)]. The most serious problem with welding metallic glass is crystallization in the molten and heat-affected zones. If the cooling rate from the liquidus temperature to the glass transition temperature is slower than the critical cooling rate of the glass formation, metallic glass rapidly transforms into intermetallic compounds, which are mostly brittle and of low strength compared with those of the amorphous. Therefore, a high energy density source, such as a laser, is well suited for welding of metallic glass. A fiber laser can focused the beam diameter to less than 100 μm. Therefore, it can produce an ultrahigh power density of the order of megawatts per square millimeter, which corresponds to the power density of a focused electron beam. Such a fiber laser has the potential for processing with low heat input, which leads to a rapid cooling rate and consequently minimizes processing risks such as crystallization and excessive enlargement of the heat-affected zone. An additional advantage of the proposed method, in comparison with electron beam welding, is that fiber lasers can operate in a vacuum-free

† Received on June 11, 2010
* Specially Appointed Assistant Professor
** Institute for Materials Research, Tohoku University
*** Tohoku University

Transactions of JWRI is published by Joining and Welding Research Institute, Osaka University, Ibaraki, Osaka 567-0047, Japan

(a)

(b)

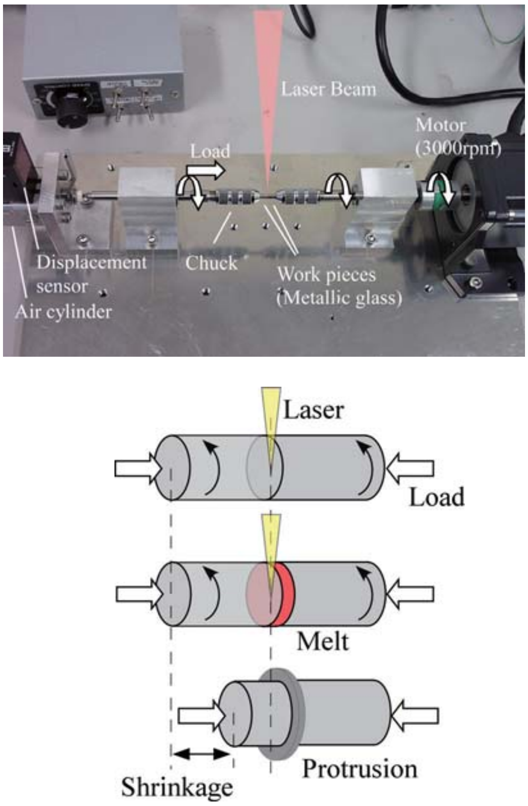

Fig. 1 (a) Laser buttwelding apparatus and (b) schematic illustration of the welding process.

(a)

(b)

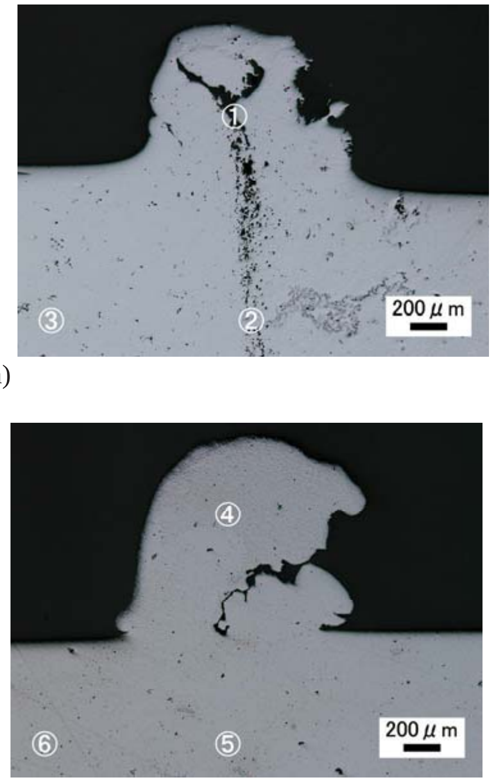

Fig. 2 Microstructures of the cross section near the protrusion welded at (a) 0.05 MPa and (b) 0.5 MPa.

environment. In this work, laser buttwelding of $Mg_{65}Cu_{25}Gd_{10}$ metallic glass is demonstrated.

2. Experimental

$Mg_{65}Cu_{25}Gd_{10}$ pre-alloy was prepared by the following procedure. Cu-Gd alloy was prepared by arc-melting a mixture of Cu and Gd together under a Ti-gettered argon atmosphere in a water-cooled copper crucible. Then the Cu-Gd alloy was alloyed with Mg in a graphite crucible in an Ar atmosphere by an induction-heating furnace. The resulting $Mg_{65}Cu_{25}Gd_{10}$ pre-alloy button was cast by the liquid quench method to form a metallic glass rod with dimension of ϕ3×75 mm. The $Mg_{65}Cu_{25}Gd_{10}$ rod was cut to a dimension of ϕ3×15 mm. The prepared $Mg_{65}Cu_{25}Gd_{10}$ metallic glass rod was welded using a fiber laser welding facility (IPG Co., Ltd., YLR-10000) with a maximum laser power of 10 kW and beam parameter product (BPP) of 4.5 mm·mrad. The laser beam was transmitted through optical fibers and focused on the specimen surface with a focal lens. The spot size at the focal position was ϕ=200 µm.

A photograph of the laser buttwelding apparatus and schematic illustration of the buttwelding process is shown in **Fig.1 (a)** and **(b)**, respectively. A pair of $Mg_{65}Cu_{25}Gd_{10}$ specimens was attached to the specimen chuck and butted together. The specimen chucks can synchronously rotate at 3000 rpm and apply a maximum pressure to the specimens of 0.5 MPa. Shrinkage of the welded specimen was measured by measuring by an LED displacement sensor. Welding was performed by irradiating the interface of the $Mg_{65}Cu_{25}Gd_{10}$ rods rotating at 3000 rpm with a laser pulse of 0.5 kW for 80 ms. Applied pressures of 0.05 MPa and 0.5 MPa were tested.

The cross-sectional surface of the joint was polished. The microstructure of the joint was analyzed with an optical microscope. The formation of a glassy phase was confirmed by micro-focused X-ray diffractometry (XRD) using Co Kα radiation. In addition, preliminary differential scanning calorimetry (DSC) measurements at a heating rate of 20 K/min were conducted to evaluate the thermal stability of the prepared $Mg_{65}Cu_{25}Gd_{10}$ metallic glass. The glass transition temperature T_g, the crystallization temperature T_x, and the liquidus temperature T_l were 423 K, 484 K, and 740 K, respectively. The strength of the joint was measured by compressive test at a strain rate of 5×10^{-4} s^{-1} for a specimen with dimensions of ϕ3×6 mm.

3. Results and Discussion

Figure 2 (a) and **(b)** show the microstructures of the cross section near the protrusion welded at pressure of 0.05 MPa and 0.5 MPa, respectively. Clear contrast with the crystalline phase was observed along the weld line in the joint welded at 0.05 MPa. No contrast was observed

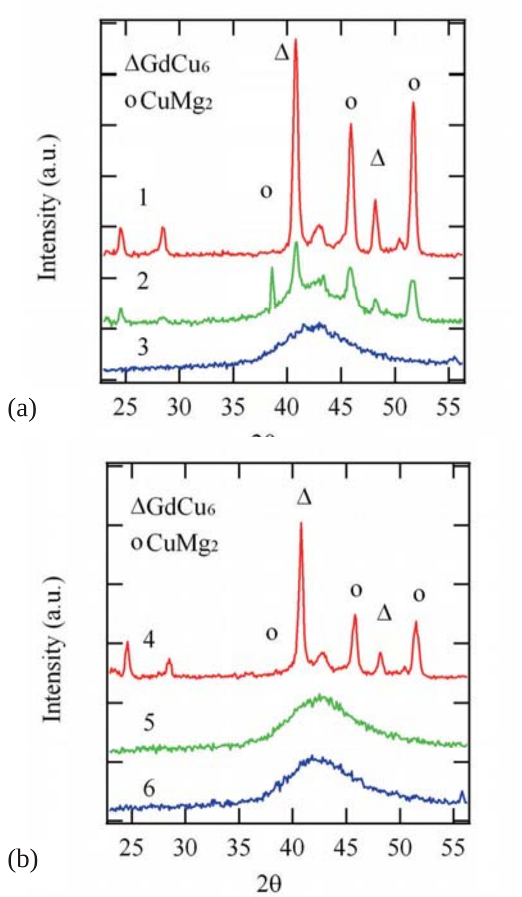

Fig. 3 Micro-focused XRD patterns at (a) positions 1, 2 and 3 in Fig. 2 (a), and (b) positions 4, 5 and 6 in Fig. 2 (b).

in the joint welded at 0.5 MPa, indicating an amorphous material. Although most of the molten region was spattered by the applied pressure and centrifugal force of the specimen rotation during laser buttwelding process, a surface protrusion with a thickness of approximately 1 mm was observed outside the joint. Neither deformation nor swelling was observed other than the protrusion. **Figure 3 (a)** and **(b)** show micro-focused XRD patterns corresponding to positions 1, 2, and 3 shown in Fig. 2 (a) and positions 4, 5, and 6 in Fig. 2 (b), respectively. The results show that the protrusion (position 1) and the center of the joint (position 2) welded at a pressure of 0.05 MPa were mainly composed of $GdCu_6$ and $CuMg_2$ intermetallic compounds. Although the protrusion (position 4) welded at a pressure of 0.5 MPa was also composed of these intermetallic compounds, the center of the joint (position 5) was amorphous, which is characterized by a halo pattern. Furthermore, the region within 3 mm of the center of the joint was also confirmed to be amorphous in each specimen (positions 3 and 6).

Figure 4 (a) shows the shrinkage of the specimen during the welding. The shrinkage proceeded in two stages. In the first stage (0-80 ms), the specimens rapidly shrank during laser irradiation. In the second stage (80-500 ms), although the laser was off, the specimens continued to shrink slightly. The shrinkage was approximately 0.2 mm and 1 mm for the specimens welded at 0.05 MPa and 0.5 MPa, respectively. After the second stage, the shrinkage was ultimately 1.3 mm and 2.9 mm for the specimens welded at 0.05 MPa and 0.5 MPa, respectively. It appeared that the shrinkage in the first stage was caused by extrusion of the molten alloy, and the shrinkage in the second stage was caused by the superplastic deformation of the supercooled liquid alloy in the heat-affected zone (HAZ). Figure 4 (b) shows an expanded view of the shrinkage during the first stage. The specimens shrank in four steps at intervals of 20 ms. The step interval corresponds to the rotation period of the specimen. Thus, the butt joint interface of $Mg_{65}Cu_{25}Gd_{10}$ was melted by the laser irradiation and rotation, and the molten alloy was extruded by the applied pressure. Undesirable crystalline phases such as $GdCu_6$ and $CuMg_2$ were removed from the joint by this extrusion. However, if the applied pressure was too small to extrude an adequate amount of molten alloy, the crystalline phases remained in the joint, as was observed at the pressure of 0.05 MPa.

Figure 5 shows the compressive stress-strain curve of

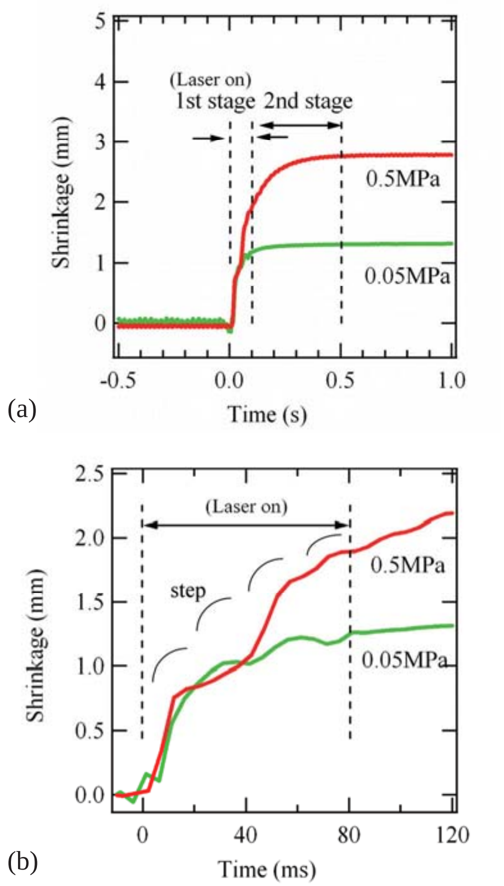

Fig. 4 (a) Shrinkage of specimen during laser buttwelding process. (b) Expanded view from 0 to 120 ms.

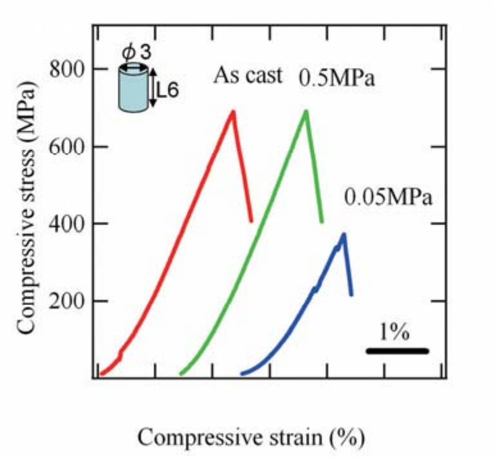

Fig. 5 Compressive stress-strain curves of as cast and welded $Mg_{65}Cu_{25}Gd_{10}$.

the as-cast $Mg_{65}Cu_{25}Gd_{10}$ and the $Mg_{65}Cu_{25}Gd_{10}$ welded at pressures of 0.05 MPa and 0.5 MPa. As indicated, the behavior of the $Mg_{65}Cu_{25}Gd_{10}$ metallic glass is strictly elastic without any macroscopic plastic deformation. The compressive fracture strength of $Mg_{65}Cu_{25}Gd_{10}$ welded at a pressure of 0.5 MPa was 690 MPa, which was the same as that of the as-cast $Mg_{65}Cu_{25}Gd_{10}$. In contrast, the specimen welded at a pressure of 0.05 MPa had a compressive fracture strength of 390 MPa. This decrease of the strength was expected since brittle intermetallic compounds such as $GdCu_6$ and $CuMg_2$ formed in the joint welded at the lower pressure.

4. Conclusions

Laser buttwelding was performed for $Mg_{65}Cu_{25}Gd_{10}$ metallic glass. When 0.5 MPa was applied to the specimens, $Mg_{65}Cu_{25}Gd_{10}$ rods were successfully welded together and maintained an amorphous structure. In contrast, when 0.05 MPa was applied, the joint contained crystalline phases composed of $GdCu_6$ and $CuMg_2$ intermetallic compounds. It was found that the applied pressure plays an important role in extruding the molten alloy and undesirable crystalline phases from the joint during laser buttwelding of $Mg_{65}Cu_{25}Gd_{10}$ metallic glass.

References

1) A. Inoue, H. Horikiri, A. Kato and T. Masumoto, Upset Deformation of Amorphous $Mg_{85}Y_{10}Cu_5$ Alloy in an Extended Supercooled Liquid Region Effectuated by Rapid Heating, Mater. Trans. JIM, 35 (1994) 79-82.
2) J. Eckert, A. Kubler and L. Schultz, Mechanically alloyed $Zr_{55}Al_{10}Cu_{30}Ni_5$ metallic glass composites containing nanocrystalline W particles, J. Appl. Phys., 85 (1999) 7112-7119.
3) A. Inoue, K. Ohtera, K. Kita, and T. Masumoto, New Amorphous Mg-Ce-Ni Alloy with High Strength and Good Ductility, Japan. J. Appl. Phys., 27 (1988) L2248-L2251.
4) A. Inoue, T. Zhang, and T. Masumoto, Zr-Al-Ni Amorphous Alloys with High Glass Transition Temperature and Significant Supercooled Liquid Region, Mater. Trans. JIM., 31 (1990) 177-183.
5) A. Peker and W. L. Johnson, A highly processable metallic glass: $Zr_{41.2}Ti_{13.8}Cu_{12.5}Ni_{10}Be_{22.5}$, Appl. Phys. Lett., 63 (1993) 2342-2344.
6) A. Inoue and J. S. Gook, Fe-Based Ferromagnetic Glassy Alloys with Wide Supercooled Liquid Region, Mater. Trans. JIM., 36 (1995) 1180-1183.
7) A. Inoue, T. Zhang, T. Itoi, and A. Takeuchi, New Fe-Co-Ni-Zr-B Amorphous Alloys with Wide Supercooled Liquid Regions and Good Soft Magnetic Properties, Mater. Trans. JIM., 38 (1997) 359-362.
8) A. Inoue, N. Nishiyama, and T. Matsuda, Preparation of Bulk Glassy $Pd_{40}Ni_{10}Cu_{30}P_{20}$ Alloy of 40 mm in Diameter by Water Quenching, Mater. Trans. JIM., 37 (1996) 181-184.
9) R. Akatsuka, T. Zhang, M. Koshiba, and A. Inoue, Preparation of New Ni-based Amorphous Alloys with a Large Supercooled Liquid Region, Mater. Trans. JIM., 40 (1999) 258-261.
10) H. Men and D. H. Kim, Fabrication of ternary Mg-Cu-Gd bulk metallic glass with high glass-forming ability under air atmosphere, J. Mater. Res., 18 (2003) 1502-1504.
11) Y. Kawamura, T. Shoji, and Y. Ohno, Welding technologies of bulk metallic glasses, J. Non-cryst. Solids, 317 (2003) 152-157.
12) Y. Kawamura and Y. Ohno, Superplastic bonding of bulk metallic glasses using friction, Scr. Mater., 45 (2001) 279-285.
13) Y. Kawamura and Y. Ohno, Superk welding of $Zr_{55}Al_{10}Ni_5Cu_{30}$ bulk metallic glasses, Scr. Mater., 45 (2001) 127-132.
14) J. Kim, D. Lee, S. Shin, and C. Lee, Phase evolution in $Cu_{54}Ni_6Zr_{22}Ti_{18}$ bulk metallic glass Nd:YAG laser weld, Mater. Sci. and Eng. A, A434 (2006) 194-201.
15) B. Li, Z. Y. Li, J. G. Xiong, L. Xing, D. Wang, and Y. Li, Laser welding of $Zr_{45}Cu_{48}Al_7$ bulk glassy alloy, J. Alloys Comp., 413 (2006) 118-121.